Quantum Chemical Studies of Three-Photon Absorption of Some Stilbenoid Chromophores

Pawel Sałek,[†] Hans Ågren,[†] Alexander Baev,*[,‡] and Paras N. Prasad[‡]

Theoretical Chemistry, Roslagstullsbacken 15, Royal Institute of Technology, AlbaNova S-106 91, Stockholm, Sweden, and Institute for Lasers, Photonics and Biophotonics, SUNY at Buffalo, Buffalo, New York 14260-3000

Received: June 22, 2005; In Final Form: September 14, 2005

Three-photon absorption of a series of donor−acceptor *trans*-stilbene derivatives is studied by means of density functional theory applied to the third-order response function and its residues. The results obtained by using different functionals are compared with experimental data for similar systems obtained from the literature. With a Coulomb attenuated, asymptotically corrected functional, the excitation energy to the first resonance state is much improved. Comparison with experiment indicates that this is the case for the three-photon cross section as well. In particular, the overestimation of the cross sections and underestimation of excitation energies offered by the density functional theory using common density functionals is corrected for. It is argued that a reliable theory for three-photon absorption in charge transfer and other chromophore systems thereby has been obtained. Further elaboration of the theory and its experimental comparison call for explicit inclusion of solvent polarization and pulse propagation effects.

1. Introduction

Novel "designer" organic compounds featuring large three-photon absorption cross sections have been of particular interest since many attractive applications exploiting high-order nonlinearity of media's response to the exciting light have been suggested.[1] These include ultrahigh-resolution biological imaging (three-photon confocal microscopy), high-efficiency upconverted lasing for infrared (IR)-to-visible upconversion, and optical power limiting where the range of radiation amenable to effective suppression can be extended to the IR region.[1] Theoretical predictions of reliable structure-to-property relations have thus become of extreme importance in providing design criteria in light of costly and time-consuming synthesis. Such predictions have usually been based on semiempirical calculations of the electronic structure of molecules. On the other hand, first principles methodologies, like Density Functional Theory (DFT), have gained much popularity over the past decade as tools capable of accurately handling relatively large systems, especially in connection with linear scaling algorithms and parallel performance. Recent progress in time-dependent DFT, or DFT response, theory applied to Kohn−Sham reference states allows for calculation of various molecular properties in an elegant and formally strict way, yet maintaining much of the efficiency of the ground-state density optimization.[2] The time-dependent DFT goes beyond the so-called adiabatic local density approximation for high-order properties, up to and including fourth order in the matter-field interaction.[2] This development has made DFT a practical approach also for three-photon absorption (3PA).

Although experimentally verified already in 1964 by Singh and Bradley,[3] 3PA is far less theoretically investigated than the two-photon absorption (TPA) analogue. In particular, the various ways of rationalizing TPA in more intuitive properties such as group symmetry, acceptor−donor strength, and dimensionality[4−12] have not been accomplished to the same extent for 3PA. Macroscopically, the cross sections for 3PA are related to the fifth-order susceptibility, $\chi^{(5)}$, which presents quite a formidable undertaking to compute even for small size systems. However, response theory allows computation of the many-photon process at the same order of perturbation as the corresponding nonlinear polarizability. Thus by examining the expressions for $\chi^{(3)}$ and $\chi^{(5)}$ at resonance conditions (i.e., $\omega = \omega_f/2$ and $\omega = \omega_f/3$) in order to identify the transition probabilities, δ^{TPA} and δ^{3PA}, one derives second and third-order transition moments, which formally can be represented by sum-over-states expressions and identified from appropriate single residues of the quadratic and cubic response functions. This greatly alleviates the theoretical calculations, in particular for 3PA.

Pure ab initio calculations for larger systems have been demonstrated in previous publication,[13] but they were confined to the Hartree−Fock noncorrelated level. As an alternative to the full calculations, one can employ so-called few-state models obtained by truncating the sum-over-states expressions. Such models have proved successful for TPA in many studies, while for 3PA a noticeable and not entirely systematic divergence has recently been predicted.[14] The disagreement between the response theory results and the few-state model approach for 3PA thus motivates other means of incorporating electron correlation in the description than applying such few-state models. Considering the size of these systems and computational tractability, the method of choice is DFT. Fortunately, the cubic response theory recently implemented in DFT, as commented above,[2] enables improvements of the predictions with a high degree of correlation. The DFT cubic response theory was also recently employed by Cronstrand et al. for three-photon calculations, comparing results from this theory with results from a hierarchy of coupled cluster methods as well as with Hartree−Fock.[15] Indeed, DFT was found to recapitulate the high-level correlation results well for the small species, while for the somewhat larger species such as donor−acceptor *trans*-stilbenes and di-thienothiophenes, there was a considerable deviation between DFT (B3LYP) and Hartree−Fock, in fact up to 2 orders

* Corresponding author e-mail: abaev@buffalo.edu.
[†] Royal Institute of Technology.
[‡] SUNY at Buffalo.

10.1021/jp0533877 CCC: $30.25
Published on Web 11/12/2005

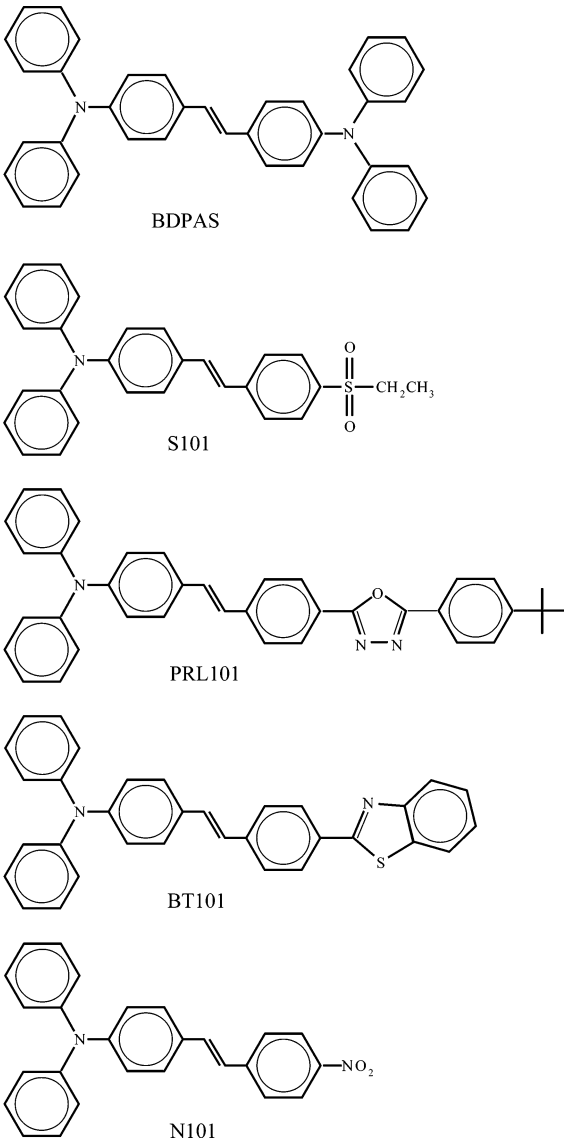

Figure 1. Chemical structures of the stilbene derivaties studied.

of magnitude in the cross section. Although the 3PA cross section is a very sensitive property, which is delicately dependent on parametrization, deviations of that magnitude are discomforting.

The purpose of the present work is 2-fold: (i) to rationalize the behavior of DFT and Hartree−Fock 3PA cross sections for a series of systematically derivatized asymmetric stilbenes (see Figure 1), utilizing some recent advances of DFT theory, and (ii) to explore how this series of molecules, which have been found to be good two-photon absorbers, performs in the three-photon case. In the following, we briefly review the essential steps of the theory and present and analyze the computed results.

2. Theory and Computation

As we address the utility of DFT for 3PA, the choice of functionals deserves some analysis. We present results from calculations using three functionals belonging to different levels of approximation. The Local Density Approximation functional (LDA) is founded on the assumption that total exchange-correlation energy is a functional of local density only. This model is valid only for slowly varying densities, and its use in chemical calculations has been limited since the electron density in all-electron calculations on ordinary molecules varies by several orders of magnitude. Still, LDA establishes a reference point for comparison of quality of further improvements. LDA functionals are improved by adding nonlocal corrections, most commonly limited to the density gradient. Such corrections establish another class of Generalized Gradient Approximation (GGA) functionals. Becke exchange functional and LYP correlation functionals belong to this group. Still, such functionals are unable to take into account global charge fluctuations. Further significant improvement can therefore be achieved by including nonlocal, fractional Hartree−Fock exchange interactions, constructing hybrid functionals. A very successful example of such a functional is the B3LYP functional consisting of 20% of HF exchange, 80% of Dirac−Slater exchange functional with 72% of Becke nonlocal exchange correction, 19% of VWN local correlation functional, and finally 81% of LYP nonlocal correlation functional.

Since its establishment in 1993, the B3LYP functional has probably become the most commonly used one due to its versatility. Further functional improvements are more challenging. While improved with respect to pure LDA or GGA functionals, one known weakness of B3LYP, or exactly of its exchange part, is that the description of long-range interactions is inadequate. In particular, it can be shown that long-range exchange should decay exactly as r^{-1}, while B3LYP accounts only for one-fifth of the interaction. This leads to such deficiencies as overestimation of the longitudinal polarizabilities of π-conjugated polyenes ("overpolarization") and underestimations of Rydberg excitation energies, oscillator strengths, and charge-transfer excitation energies (i.e., all excitation processes connected with long-distance charge redistribution). However, using 100% of Hartree−Fock exchange, which would have proper long-range behavior, deteriorates many of other properties. Hence such a functional would not provide a general improvement with respect to B3LYP. It is in clear that these properties of the commonly used B3LYP functional are of concern for applications on charge-transfer excitations, be it of one- or multiphoton nature.

A Coulomb-Attenuating Method has been proposed to address this issue.[16,17] The method is based on accounting for all the short-range interactions in exactly the same way as the B3LYP functional does. At the same time, the fraction of HF exchange for the long-range interactions is enhanced. This has been achieved by an Ewald split of the r_{12}^{-1} operator where the error function is used to perform the switching between the short- and the long-range regions, as given by eq 1:

$$\frac{1}{r_{12}} = \frac{1 - \alpha - \beta\,\mathrm{erf}(\mu r_{12})}{r_{12}} + \frac{\alpha + \beta\,\mathrm{erf}(\mu r_{12})}{r_{12}} \qquad (1)$$

The first term is next approximated with help of a functional, and the second one weighs HF exchange. Such a split makes it possible to account with α fraction of HF exchange for short-range interactions and $\alpha + \beta$ fraction for long range. In the original paper,[18] $\alpha = 0.19$, $\beta = 0.46$, and $\mu = 0.33$ were recommended; these values are used in this paper as well. Such parametrization will provide 65% of the expected long-range interaction. Another parametrization $\alpha = 0.19$ and $\beta = 0.61$ accounting for 80% of the asymptotic long-range interaction was also investigated in ref 16 but was found to slightly less successfully recover other molecular parameters.

Finally, to compute the electronic structure of the compounds of interest (Figure 1), we employed the Dalton[19] and the Gaussian codes.[20] The ground-state geometries for all compounds were optimized by making use of the Gaussian98 code[20]

at the DFT B3LYP/6-31G* level. Three-photon transition matrix elements were evaluated by means of DFT cubic response (CR) function recently implemented in the Dalton program.[15] DFT/CR calculations were done with the hybrid functionals LDA, B3LYP, and CAM-B3LYP and with the 6-31G* basis set. We also computed three-photon transition matrix elements in the framework of random phase approximation (time-dependent Hartree−Fock method) in order to make comparison with the DFT results.

3. Results and Discussion

3.1. Linear Absorption. To make comparison of the computed data with the experimental ones, we first analyzed the linear absorption spectra of all molecules, including a reference molecule called BDPAS[21] for which both linear and 3PA cross sections are measured. We were primarily interested in the molar extinction coefficients and positions of the absorption bands. The molar extinction coefficient, ϵ ($cm^{-1}\cdot M^{-1}$), can be evaluated with help of the conventional expression for the one-photon absorption (OPA) cross section:

$$\epsilon = \frac{\omega}{3\epsilon_0 c\hbar}\frac{d_{S_1S_0}^2\Gamma}{\Gamma^2 + (\omega - \omega_{10})^2} \times 10N_A \qquad (2)$$

where orientational averaging is taken into account and SI units are used. Here $d_{S_1S_0}$ is the transition matrix element, ω is the frequency of the exciting radiation, $\omega_{10} = (E_1 - E_0)/\hbar$ is the transition frequency, Γ is the homogeneous broadening of molecular transitions, and N_A is the Avogadro number.

To evaluate the molar absorption coefficient by means of the above equation, we need to choose the value of the damping factor Γ, which is often set to 0.1 eV for chromophore solutions.[22] However, the use of this value in eq 2 results in strongly overestimated absorption coefficients as compared to the experimental values. The reason for this is that we neglect vibrational broadening of the absorption band in eq 2. Apparently, the transition matrix element $d_{S_1S_0}$ in the one-mode approximation is a product of the electronic matrix element and the Franck−Condon amplitude, $\langle 0|f\rangle$, between the zero-point vibrational level (assuming low-temperature approximation) of the ground state and the vibrational levels of the first excited electronic state. Simulating the experimental absorption profile thus requires to perform summation of the absorption amplitudes over vibrational levels of the excited electronic state.

As a matter of fact, for larger systems the problem of evaluating the generalized Franck−Condon amplitude is far from trivial. Therefore, we decided to evaluate the values of the absorption coefficients making use of the experimental broadening. According to ref 23, the full width at half-maximum (FWHM) of the first linear absorption band of the molecules under consideration is about 0.5−0.7 eV. However, it turns out that just changing the value of Γ to the experimental broadening in eq 2, which assumes a Lorentzian profile of the absorption bands, does not very well reproduce the experimental shapes. Therefore, as in ref 26, to provide a closer agreement with the experiment, we recast eq 2 in the form of a Gaussian function which better fits the experimentally observed absorption profiles:

$$\epsilon = \frac{\omega}{3\epsilon_0 c\hbar}\frac{d_{S_1S_0}^2 e^{-\frac{(\omega - \omega_{10})^2}{\Delta^2}}}{\Delta} \times 10N_A \qquad (3)$$

TABLE 1: Molar Extinction Coefficients (10^4 $cm^{-1}\cdot M^{-1}$), Excitation Energies (eV), and Gaussian Width Parameters (eV) of BDPAS, S-101, PRL-101, BT-101, and N-101 (Gaussian98 B3LYP data)

molecule	ϵ^a	$\Delta E_{DFT}{}^b$	ϵ_{exp}	$\Delta E_{exp}{}^c$	Δ
BDPAS	10.87	2.95	5.9	3.21	0.304
S-101	6.54	2.93	2.6	3.22	0.324
PRL-101	9.05	2.77	4.1	3.11	0.328
BT-101	7.81	2.72	4.5	3.10	0.361
N-101	3.49	2.50	2.4	2.82	0.437

[a] See eq 3. [b] Absorption at the equlibrium ground-state geometry. [c] Ref 23.

TABLE 2: Calculated 3PA Cross Sections (10^{-81} $cm^6\cdot s^2$) and Excitation Energies (eV) of BDPAS, S-101, PRL-101, BT-101, and N-101

	HF		LDA		B3LYP		CAM-B3LYP		exp[23]
molecule	$\sigma_{3PA}{}^a$	ΔE^b	$\sigma_{3PA}{}^a$	ΔE^b	$\sigma_{3PA}{}^a$	ΔE^b	$\sigma_{3PA}{}^a$	ΔE^b	ΔE^c
BDPAS	6.67	3.98	228.63	2.43	123.99	2.95	37.76	3.48	3.21
S-101	6.33	4.04	108.24	2.38	107.74	2.93	39.09	3.53	3.22
PRL-101	12.30	3.85	1093.30	2.14	501.76	2.77	89.02	3.40	3.11
BT-101	12.13	3.79	671.71	2.12	447.36	2.72	90.16	3.36	3.10
N-101	8.55	3.90	155.59	1.87	231.80	2.51	69.16	3.32	2.82

[a] Calculated with Δ from Table 1. [b] Absorption at the equlibrium ground-state geometry. [c] The peak value of linear absorption spectrum.

where $\Delta = \mathrm{FWHM}/2\sqrt{\ln 2}$ and FWHM is that of the experimental absorption profile.

The results of our analysis of the OPA spectra, based on Gaussian98 B3LYP/6-31G* data, are collected in Table 1. As one can see, the absorption coefficients are still overestimated, and the peak positions of the bands are red-shifted. The reason for this lies in the nature of the B3LYP functional (see the discussion in Section 3.4).

3.2. Three-Photon Absorption. The 3PA cross section is related to the fifth-order molecular susceptibility, $\chi^{(5)}$. Though being a fifth-order property, the 3PA cross section is also available through the third-order transition matrix elements:

$$T_{abc} = \sum \mathscr{P}_{a,b,c} \sum_{n,m} \frac{\langle 0|\mu_a|m\rangle\langle m|\mu_b|n\rangle\langle n|\mu_c|f\rangle}{(\omega_m - 2\omega_f/3)(\omega_n - \omega_f/3)} \qquad (4)$$

where $\sum\mathscr{P}_{a,b,c}$ denotes permutations with respect to the Cartesian indices a, b, and c. We evaluate the 3PA cross section, $\sigma^{(3)}$, by making use of the formulas that relate this quantity to the three-photon transition probability, δ_{3p}, and T_{abc}:[24]

$$\sigma^{(3)} = \frac{\hbar\omega^3}{4c^3\epsilon_0{}^3\Gamma}\delta_{3p}^L \quad \delta_{3P}^L = \frac{1}{35}(3\delta_F + 2\delta_G)$$
$$\delta_F = \sum_{ijk} T_{iij}T_{kkj} \quad \delta_G = \sum_{ijk} T_{ijk}T_{ijk} \qquad (5)$$

where λ is the wavelength of the incoming photon. The three-photon transition probability, δ_{3P}^L, for linearly polarized light is averaged over molecular orientations. Apparently, the completeness should result in the same vibrational profile for one-photon and three-photon absorption. Therefore, it seems to be a reasonable approximation to use the same Δ as in the case of linear absorption instead of the Γ in eq 5. The results of the calculations are collected in Table 2.

Let us now discuss in more detail the method we use for computing the third-order transition matrix elements. In the response formalism, the infinite summation in eq 4 corresponds to the single residue of the cubic response function. Even though

the response approach represents a significant simplification, it remains computationally demanding for three-photon absorption, and the third-order transition moments are often obtained at the random phase approximation (RPA) level, where the cubic response theory is applied to a singe-determinant self-consistent field (SCF) reference state.[25] Recently, the DFT was derived and implemented for the cubic response function.[15] The working expressions are derived from an explicit exponential parametrization of the density operator and from the Ehrenfest principle. A general aspect of the theory, relevant for the present work, is that it generalizes previous time-dependent approaches in that arbitrary functionals can be chosen for the perturbed densities (energy derivatives or response functions). At the same time, the theory retains the adiabatic approximation, implying that the time dependency of the functional is obtained only implicitly, through the time dependence of the density itself rather than through the form of the exchange-correlation functional. Thus, the response of the density can always be obtained using the stated density functional, or optionally different functionals can be applied for the unperturbed and perturbed densities, even different functionals for different response order. In particular, general density functionals beyond the local density approximation can be applied, such as hybrid functionals with exchange-correlation at the generalized gradient-approximation level and fractional exact Hartree−Fock exchange. The applicability of these functionals for both the linear and the nonlinear responses of the density adds an important functionality of DFT for investigation of a sensitive property like 3PA and its parametrical dependence.

3.3. Comparison of HF, LDA, B3LYP, and CAM-B3LYP Results. In this application of DFT to 3PA, we have tested the commonly available and extensively used functionals (LDA and B3LYP) and the newly derived functional CAM-B3LYP. Of course, there are many other types of available functionals streamlined for various molecular features. To the latter we can refer, for instance, to the PBE0 functional, with 25% "exact" exchange, which can provide accurate excitation spectra.[28] Also, so-called orbital optimized functionals (OLYP[29]) seem to constitute a promising update of B3LYP. In that context, it is also relevant to point out that, for heavily delocalized systems, commonly used functionals show inappropriate asymptotic dependences of excitation energies[30] and polarizabilities[31,32] and that pure and hybrid DFT functionals may provide qualitatively and quantitatively incorrect results for large compounds due to "overpolarization". We indeed find strong enhancement of the 3PA cross sections with respect to Hartree−Fock for LDA and B3LYP functionals (Table 2, see also work of Cronstrand et al. on B3LYP[15]). We keep in mind that the treatment of charge-transfer excitations is also of concern using local density functionals. Thus, we believe that asymptotically corrected CAM-B3LYP functional will cope with DFT overpolarization for 3PA, as well as for linear charge-transfer spectra. The "true" 3PA cross section value is then between, roughly 1 order of magnitude larger than HF and 1 order of magnitude smaller than LDA/B3LYP. Indeed, the asymptotically corrected functional CAM-B3LYP delivers cross sections that seem to fit this prediction, making us hold the CAM-B3LYP values as plausible.

Experimental data on 3PA of the compounds studied are not available yet. However, there are similar charge-transfer organic molecules, in particular stilbene-based dendrimers, for which the 3PA cross sections have been reported.[27] For example, for the donor−donor stilbenoid chromophore BDPAS the 3PA cross section was reported to be 5×10^{-81} $cm^6 \cdot s^2$ (see ref 27). Our calculations with the CAM-B3LYP functional give very good agreement with the experiment when it comes to excitation energy and poorer agreement for the 3PA cross section, although this value is much improved in comparison with LDA and B3LYP results (see Table 2). We have to note here that pulse and saturation effects result in an effective decrease of the 3PA cross section values measured at high pulse peak intensities, something that calls for a thorough scrutiny of the experimental conditions of the measurements and modeling of such effects. These points are further commented upon in the concluding section of the paper. Considering the very delicate nature of the three-photon effect, being influenced by a number of circumstances, we consider the CAM-B3LYP improvement of the cross section as quite substantial.

All in all, it seems that the CAM-B3LYP calculations give the best agreement for both the 3PA cross-sections and the excitation energies with the experimental data. The B3LYP functional is found to underestimate the energies and strongly overestimate the 3PA cross sections. This was, however, expected from our calculations of the TPA cross sections for the same series.[26] Apparently, the overestimation of the cross sections should be even more prominent for calculations with the LDA functional, because it does not contain nonlocal exchange terms. Indeed, our calculations confirmed this fact. As expected, the TDHF method overestimates the vertical excitation energies and, hence, should underestimate the cross sections, although the absolute values of the 3PA cross sections are close to the experimentally reported values for similar system.[27]

In analyzing the results of Table 2, we repeat the observation of Cronstrand et al.[15] that DFT cross sections with common functionals (LDA and B3LYP) can overestimate the HF cross section by as much as 2 orders of magnitude. Thus, this does not only reflect the sensitive nature of the 3PA cross section itself but was conjectured in ref 15 to be due to the overpolarization nature of these functionals, simultaneously with a general underestimation of HF total cross sections and of HF intermediate excited-state one-photon transition moments. As noted recently,[33] this can also induce a problematic charge distribution of the excited charge transfer state. We have already noted that the excitation energy is underestimated by LDA and B3LYP but is overestimated by roughly the same amount by Hartree−Fock. We also have to underline that as the compounds are measured in solution, there should in general be small red shifts (a few tenths of an eV) of the predicted excitation energies. We refer to ref 34 where these shifts have been addressed for two-photon excitation of larger charge-transfer chromohores. We thus find a reasonable agreement of CAM-B3LYP concerning both the magnitude and the relative size of the excitation energies.

3.4. Ordering of the Compounds. In this paper, we were also interested in comparing the ordering of the compounds with respect to their 3PA cross section values with the ordering obtained in ref 26 for the TPA cross sections. The observed systematic increase of the TPA cross sections was attributed to systematic increase of the electron acceptor strength.

For calculations with LDA and B3LYP functionals and the split valence 6-31G* basis set, the ordering obtained for the values of the 3PA cross sections is exactly the same we observed for the TPA cross sections computed at the B3LYP/6-31G* level,[26] namely, S-101 < N-101 < BT-101 < PRL-101. The ordering changes for calculations with the CAM-B3LYP functional and for the TDHF calculations. In this case two compounds are interchanged and the ordering becomes S-101 < N-101 < PRL-101 < BT-101. It is interesting that

this ordering coincides with the ordering obtained for the TPA cross sections at the B3LYP level with the use of a larger double-ζ basis set cc-pVDZ instead of the split-valence 6-31G* basis set.

To figure out the reason for the observed ordering with respect to the values of the 3PA cross sections, we analyzed the strongest possible 3PA virtual channels focusing on the structure of the largest 3PA matrix element, T_{xxx}. We presume that the initial state is the ground state S_0 and that the final state is the lowest-lying excited singlet state S_1. For all compounds, the photon energy detunings from the transition energies are about the same, so we can exclude them from our consideration. Applying the simple few-state picture we can identify two strong 3PA channels: $\langle S_0|S_3\rangle\langle S_3|S_2\rangle\langle S_2|S_1\rangle$ and $\langle S_0|S_2\rangle\langle S_2|S_1\rangle[\langle S_1|S_1\rangle - \langle S_0|S_0\rangle]$. A simple analysis of the dipole transition matrix elements indicates that the latter virtual channel is indeed the strongest one. The ordering of the compounds thus becomes S-101 < BT-101 < N-101 < PRL-101 with two molecules (N-101 and BT-101) interchanged. However, the difference between the absolute values of the 3PA matrix elements for these two compounds is tiny, which implies that some other three-photon virtual channels contribute to the matrix element, producing the ordering obtained by means of the cubic response calculations. Finally, our analysis of 3PA virtual channels showed that the increase of the electron acceptor strength associated with large difference between the dipole moments of the ground and charge-transfer states of molecules is responsible for systematic increase of the 3PA cross sections as in the case of the TPA cross sections.

4. Conclusions and Further Work

We have applied response theory at the DFT level to calculations of 3PA probabilities of a series of stilbenoid chromophores. We have compared the results obtained with several functionals, also hybrid functionals, including the newly implemented Coulomb-attenuated functional CAM-B3LYP, with reported experimental data for similar systems. According to our calculations, the CAM-B3LYP functional provides the best agreement with experimentally obtained values for 3PA cross sections and excitation energies and resolves a previously observed, discomforting, size-dependent deviation between the Hartree−Fock and the DFT for charge-transfer species. The comparison of the performance for each functional leads to the point where we can establish a theory that is credible for predictions of 3PA sections and, therefore, for the design of highly effective three-photon materials.

Of course, we should also recall that the 3PA cross sections are environment and solvent dependent. Recent calculations in the two-photon case show quite a sizable increase of the cross section due to the reaction field of the medium polarization.[38] Our implementation of the polarizable continuum model (PCM) indicated that polarization effects can lead to a significant, up to a factor of 2, enhancement of the TPA cross section for strong charge-transfer systems such as nitro-amino−*trans*-stilbene and also for corresponding donor−donor and acceptor−acceptor systems. This is natural since the dielectric medium will stabilize the charge polarization of the charge-transfer states. We can expect a general increase of the 3PA cross section as well, something that we will study using a coming implementation of PCM with cubic response theory. Also, when comparing the calculated data with the experimental ones, we must keep in mind the dynamics of the 3PA process itself, and the competition with stepwise processes under the conditions of a measurement. A primary solvent effect will indeed be to dephase the excited state, leading to an altered and enhanced role of the stepwise off-resonant processes with respect to the coherent process. As shown in ref 35, it is the stepwise three-photon process that may compete with the coherent three-photon process. To further scrutinize comparison of the computed results with experiment, one thus needs to augment the theoretical treatment with classical pulse propagation where the competing processes and the desaturation of levels are properly taken into account.

Through ongoing development of computational algorithms, like linear scaling, density fitting, and sparse matrix algebra, we foresee a further widening of the applicability of the theory to 3PA and therefore its utility as an experimental aid both in the synthesis and the characterization steps of production of new three-photon materials. As discussed, a further scrutiny of the experimental−theoretical comparisons will be obtained by considering reaction-field effects due to the solvent polarization, excited-state dephasing and stepwise three-photon contributions. In general, we are moving toward combinatory approaches in which quantum chemistry is combined with classical pulse propagation[36] and/or with molecular dynamics simulation.[37] The first type of combined approach allows to estimate the nonlinear effects in optical transmission from cross sections of the three-photon processes and from consideration of propagation effects, saturation, and pulse effects. Such an approach accounts simultaneously for the coherent one-step and incoherent stepwise multiphoton absorption as well as for off-resonant excitations even when resonance conditions prevail. This becomes important in the nonlinear regime. The other type of combined approach, quantum chemistry with molecular dynamics, allows the study of temperature and pressure effects and also cooperative effects, like pooling, aggregation, and loading, on the macroscopic outcome of the nonlinear effect. The field is thus certainly rich, with room for much research.

Acknowledgment. The authors are grateful to Marek Samoc for helpful advice and discussion. P.S. acknowledges Trygve Helgaker (University of Oslo) and Nicholas Handy (Cambridge University) for collaboration on the CAM-B3LYP functional, which is here proven essential for studies of three-photon charge transfer materials. A.B. thanks the Swedish Research Council and the Swedish Foundation for International Cooperation in Research and Higher Education for a postdoctoral fellowship. The research at Buffalo was supported by NSF Grant DMR 0307282 from the NSF division of Materials Research International Collaboration program. We also acknowledge SSF, the Swedish Foundation for Strategic Research, which is the Swedish counterpart of the NSF collaboration program and also supported this project.

References and Notes

(1) He, G. S.; Prasad, P. N. *Proc. SPIE* **2003**, *No. 5211*, 1.

(2) Salek, P.; Vahtras, O.; Helgaker, T.; Ågren, H. *J. Chem. Phys.* **2002**, *117*, 9630.

(3) Singh, S.; Bradley, L. T. *Phys. Rev. Lett.* **1964**, *12*, 612.

(4) Wang, C. K.; Macak, P.; Luo, Y.; Ågren, H. *J. Chem. Phys.* **2001**, *114*, 9813.

(5) Chung, S.-J.; Kim, K.-S.; Lin, T.-C.; He, G. S.; Swiatkiewitz, J.; Prasad, P. N. *J. Phys. Chem. B* **1999**, *103*, 10741.

(6) Macak, P.; Luo, Y.; Norman, P.; Ågren, H. *J. Chem. Phys.* **2000**, *113*, 7055.

(7) Norman, P.; Luo, Y.; Ågren, H. *J. Chem. Phys.* **1999**, *111*, 7758.

(8) Luo, Y.; Norman, P.; Macak, P.; Ågren, H. *J. Phys. Chem. A* **2000**, *104*, 4718.

(9) Cronstrand, P.; Luo, Y.; Ågren, H. *J. Chem. Phys.* **2002**, *117*, 11102.

(10) Zojer, E.; Beljonne, D.; Kogej, T.; Vogel, H.; Marder, S. R.; Perry, J. W.; Brdas, J. L. *J. Chem. Phys*. **2002**, *116*, 3646.

(11) Beverina, L.; Fu, J.; Leclercq, A.; Zojer, E.; Pacher, P.; Barlow, S.; Van Stryland, E. W.; Hagan, D. J.; Bredas, J. L.; Marder, S. R. *J. Am. Chem. Soc.* **2005**, *127*, 7282.

(12) Anemian, R.; Morel, Y.; Baldeck, P. L.; Paci, B.; Kretsch, K.; Nunzi, J. M.; Andraud, C. *J. Mater. Chem*. **2003**, *13*, 2157.

(13) Cronstrand, P.; Norman, P.; Luo, Y.; Ågren, H. *Chem. Phys. Lett*. **2003**, *375*, 233.

(14) Cronstrand, P.; Norman, P.; Luo, Y.; H. Ågren, H. *J. Chem. Phys.* **2004**, *121*, 2020.

(15) Cronstrand, P.; Jansik, B.; Jonsson, D.; Luo, Y.; Ågren, H. *J. Chem. Phys.* **2004**, *121*, 9239.

(16) Yanai, T.; Tew, D. P.; Handy, N. C. *Chem. Phys. Lett*. **2004**, *393*, 51.

(17) Peach, M. J. G.; Helgaker, T. U.; Salek, P.; Keal, T.; Lutnaes, O.; Tozer, D. J.; Handy, N. C. *Phys. Chem. Chem. Phys.* (in press).

(18) Tawada, Y.; Tsuneda, T.; Yanagisawa, S.; Yanai, T.; Hirao, K. *J. Chem. Phys*. **2004**, *120*, 8425.

(19) Helgaker, T.; Jensen, H. J. Aa.; Jorgensen, P.; Olsen, J.; Ruud, K.; Ågren, H.; Auer, A. A.; Bak, K. L.; Bakken, V.; Christiansen, O.; Coriani, S.; Dahle, P.; Dalskov, E. K.; Enevoldsen, T.; Fernandez, B.; Haettig, C.; Hald, K.; Halkier, A.; Heiberg, H.; Hettema, H.; Jonsson, D.; Kirpekar, S.; Klopper, W.; Kobayashi, R.; Koch, H.; Mikkelsen, K. V.; Norman, P.; Pedersen, T. M.; Packer, M. J.; Rinkevicius, Z.; Rudberg, E.; Ruden, T. A.; Salek, P.; Sanchez, A.; Saue, T.; Sauer, S. P. A.; Schimmelpfennig, B.; Sylvester-Hvid, K. O.; Taylor, P. R.; Vahtras, O. *DALTON, a molecular electronic structure program*, release 2.0; 2005 (http://www.kjemi.uio.no/software/dalton/dalton.html).

(20) Frisch, M. J.; Trucks, G. W.; Schlegel, H. B.; Scuseria, G. E.; Robb, M. A.; Cheeseman, J. R.; Zakrzewski, V. G.; Montgomery, J. A., Jr.; Stratmann, R. E.; Burant, J. C.; Dapprich, S.; Millam, J. M.; Daniels, A. D.; Kudin, K. N.; Strain, M. C.; Farkas, O.; Tomasi, J.; Barone, V.; Cossi, M.; Cammi, R.; Mennucci, B.; Pomelli, C.; Adamo, C.; Clifford, S.; Ochterski, J.; Petersson, G. A.; Ayala, P. Y.; Cui, Q.; Morokuma, K.; Malick, D. K.; Rabuck, A. D.; Raghavachari, K.; Foresman, J. B.; Cioslowski, J.; Ortiz, J. V.; Stefanov, B. B.; Liu, G.; Liashenko, A.; Piskorz, P.; Komaromi, I.; Gomperts, R.; Martin, R. L.; Fox, D. J.; Keith, T.; Al-Laham, M. A.; Peng, C. Y.; Nanayakkara, A.; Gonzalez, C.; Challacombe, M.; Gill, P. M. W.; Johnson, B. G.; Chen, W.; Wong, M. W.; Andres, J. L.; Head-Gordon, M.; Replogle, E. S.; Pople, J. A. *Gaussian 98*, revision A.9; Gaussian, Inc.: Pittsburgh, PA, 1998 (http://www.gaussian.com).

(21) Ehrlich, J. E.; Wu, X. L.; Lee, I.-Y. S.; Hu, Z.-Y.; Röckel, H.; Marder, S. R.; Perry, J. W. *Opt. Lett.* **1997**, *22*, 1843.

(22) Rumi, M.; Ehrlich, J. E.; Heikal, A. A.; Perry, J. W.; Barlow, S.; Hu, Zh.; McCord-Maughon, D.; Parker, T. C.; Rockel, H.; Thayumanavan, S.; Marder, S. R.; Beljonne, D.; Bredas, J. L. *J. Am. Chem. Soc*. **2000**, *122*, 9500.

(23) Lin, T.-C.; He, G. S.; Prasad, P. N.; Tan, L. S. *J. Mater. Chem*. **2004**, *14*, 982.

(24) McCLain, W. M. *J. Chem. Phys*. **1972**, *57*, 2264.

(25) Norman, P.; Jonsson, D.; Vahtras, O.; Ågren, H. *Chem. Phys*. **1996**, *203*, 23.

(26) Baev, A.; Prasad, P. N.; Samoc, M. *J. Chem. Phys.* **2005**, *122*, 224309.

(27) Drobizhev, M.; Karotki, A.; Kruk, M.; Dzenis, Yu.; Rebane, A.; Suo, Z.; Spangler, C. W. *J. Phys. Chem. B* **2004**, *108*, 4221.

(28) Adamo, C.; Scuseria G. E.; Barone, V. *J. Chem. Phys.* **1999**, *111*, 2889.

(29) Baker, J.; Pulay, P. *J. Chem. Phys.* **2002**, *117*, 1441.

(30) Cai, Z. L.; Sendt, K.; Reimers, J. R. *J. Chem. Phys.* **2002**, *117*, 5543.

(31) Champagne, B.; Perpète, E. A.; van Gisbergen, S. J. A.; Baerends, E. J.; Snijders, J. G.; Soubra-Ghaoui, C.; Robins, K. A.; Kirtman, B. *J. Chem. Phys.* **1998**, *109*, 10489.

(32) Champagne, B.; Perpète, E. A.; Jacquemin, D.; van Gisbergen, S. J. A.; Baerends, E. J.; Soubra-Ghaoui, C.; Robins, K. A.; Kirtman, B. *J. Phys. Chem. A* **2000**, *104*, 4755.

(33) Rubio-Pons, O.; Salek, P.; Luo, Y.; Ågren, H. Manuscript in preparation.

(34) Rudberg, E.; Salek, P.; Helgaker, T.; Ågren, H. *J. Chem. Phys.* **2005**, *00*, 000.

(35) Baev, A.; Gel'mukhanov, F.; Rubio-Pons, O.; Cronstrand, P.; Ågren, H. *J. Opt. Soc. Am. B* **2004**, *21*, 384.

(36) Baev, A.; Gel'mukhanov, F.; Kimberg, V.; Ågren, H. *J. Phys. B: At. Mol. Opt. Phys.* **2003**, *36*, 3761.

(37) Tu, Y.; Luo, Y.; Ågren, H. *J. Phys. Chem. B.* **2005**, *109*, 16730.

(38) Frediani, L.; Rinkevicius, Z.; Ågren, H. *J. Chem. Phys.* **2005**, *122*, 244104.